



AIAA 98-2279

**VALIDATION OF AN IMPEDANCE
REDUCTION METHOD IN FLOW**

Willie R. Watson, Michael G. Jones and
Tony L. Parrott
NASA Langley Research Center
Hampton, VA

**4th AIAA/CEAS
Aeroacoustics Conference**
June 2-4, 1998/Toulouse, France

VALIDATION OF AN IMPEDANCE EDUCATION METHOD IN FLOW

Willie R. Watson*, Michael G. Jones† and Tony L. Parrott‡
 NASA Langley Research Center
 Hampton, VA

Abstract

This paper reports results of a research effort to validate a method for educating the normal incidence impedance of a locally reacting liner, located in a grazing incidence, nonprogressive acoustic wave environment with flow. The results presented in this paper test the ability of the method to reproduce the measured normal incidence impedance of a solid steel plate and two soft test liners in a uniform flow. The test liners are known to be locally reacting and exhibit no measurable amplitude-dependent impedance nonlinearities or flow effects. Baseline impedance spectra for these liners were therefore established from measurements in a conventional normal incidence impedance tube. A key feature of the method is the expansion of the unknown impedance function as a piecewise continuous polynomial with undetermined coefficients. Stewart's adaptation of the Davidon-Fletcher-Powell optimization algorithm is used to educate the normal incidence impedance at each Mach number by optimizing an objective function. The method is shown to reproduce the measured normal incidence impedance spectrum for each of the test liners, thus validating its usefulness for determining the normal incidence impedance of test liners for a broad range of source frequencies and flow Mach numbers.

Nomenclature

$[A(\beta_{Iq})], [AB]$	block-tridiagonal matrices
$[A_I], [B_I], [C_I]$	major blocks in $[A(\beta_{Iq})]$
$[A^{[I,J]}]$	local element matrix
a, b	length and height of an element
$[a_I], [b_I], [c_I]$	minor blocks in $[A(\beta_{Iq})]$

*Senior Research Scientist, Aerodynamic and Acoustics Methods Branch, Fluid Mechanics and Acoustics Division

†Research Scientist, Structural Acoustics Branch, Fluid Mechanics and Acoustics Division

‡Senior Research Scientist, Structural Acoustics Branch, Fluid Mechanics and Acoustics Division

Copyright ©1998 by the American Institute of Aeronautics and Astronautics, Inc. No copyright is asserted in the United States under Title 17, U.S. Code. The U.S. Government has a royalty-free license to exercise all rights under the copyright claimed herein for government purposes. All other rights are reserved by the copyright owner.

c_0, ρ_0	ambient sound speed and density
dA	differential of cross-sectional area
$E(x, y)$	field-equation error function
$f_q(x, a)$	one-dimensional basis functions
$\{F\}$	vector containing source effects
H, L	height and length of the duct
i	$\sqrt{-1}$
k	ω/c_0 , free-space wave number
L_1, L_2	leading and trailing edge of liner
M, N	total number of transverse and axial nodes
N_I	two-dimensional basis
m	number of upper wall measurement points
M_0	u_0/c_0 , centerline Mach number
$p(x, y)$	acoustic pressure at (x, y)
$p_s(y)$	source and reference pressure
$p_{FE}(x_l; \beta_{Iq})$	finite-element wall pressure
u, v	axial and transverse velocity
u_0	flow speed in axial direction
x, y, z	cartesian coordinates
x_l	upper wall measurement location
$\beta(x)$	$1/\zeta(x)$, wall admittance
$\zeta(x), \zeta_{\text{exit}}(y)$	wall and exit impedance, normalized with $\rho_0 c_0$
$\psi(\beta_{Iq})$	objective function
κ, σ	conductance and susceptance
ω	angular frequency
$ $	absolute value
$\{\Phi\}$	global vector of acoustic pressures
Φ_I	nodal value of acoustic pressures
$\{\Phi^{[I,J]}\}$	local vector of acoustic pressures
subscripts:	
I, J	node counters for axial direction
	transverse direction of the duct
m	number of wall measurement points
q	1...4
superscripts:	
T	matrix transposition

Introduction

Efficient duct treatments for broadband acoustic noise suppression remain critical to the development of environmentally acceptable commercial aircraft in the next century. To this end, an accurate knowledge of duct-treatment impedance is a critical design parameter. Validation of liner impedance prediction models for grazing-flow is commonly accomplished in a flow duct that provides grazing flow/grazing incidence sound on a test liner. From appropriate measurements the “normal incidence impedance” in a grazing-incidence and grazing-flow environment and for locally reacting test materials can, in theory, be deduced. Depending on accuracy/precision required, there are several methods or approaches for accomplishing this education process. The simplest approach, the so-called infinite-wave-guide method, relies on the measurement of the propagation constant of an assumed single, unidirectional propagating mode^{1,2,3} which is directly related to the normal incidence impedance of the test specimen by means of a modal solution. In real facilities, sufficiently idealized test conditions (i.e., unidirectional, single propagating mode) are rarely attained. Additionally, should the test liner impedance be nonuniform or the flow Mach number sufficiently high, added wave field complexity results from either energy scattering into higher order modes or end reflections. While these may be desirable conditions to achieve more efficient, broadband absorbing structures, they are complicating features that cannot be handled by the infinite-wave-guide method for impedance determination.

Two recent papers presented results from a finite-element-based contour deformation method^{4,5} for educing the uniform impedance of an acoustic material located in a no-flow duct carrying a nonprogressive multimodal sound field. The contour deformation method was replaced by a more efficient optimization algorithm and the method was extended and validated for variable impedance liners.⁶ In keeping with increasing realism of this validation process, the next step is to incorporate the convective flow effects. The purpose of this paper is to extend the impedance eduction method⁶ to include the convective effects of a flow. A key element of a validation exercise is to compare educed admittance values in flow to those measured at normal incidence with no flow. To accomplish this goal, special care is taken to choose test liners that are demonstrably locally reacting, whose normal incidence impedance exhibited no measurable amplitude-dependent behavior, and where the convective effects of the grazing flow are minimal.

Problem Description

The two-dimensional test region depicted in figure 1 is spanned by x and y coordinates. The region is L units long with the source and exit planes at $x = 0$ and $x = L$, respectively. It should be noted that the mks system of measurement is used throughout this manuscript. Measured inputs at the source and exit planes are the source pressure $p_s(y)$ and the exit impedance $\zeta_{\text{exit}}(y)$, respectively. A total of m points are located at $x = x_1, x_2, x_3, \dots, x_m$ along the rigid upper wall, at which the acoustic pressures are measured. The test liner is the part of the otherwise rigid bottom wall between $L_1 \leq x \leq L_2$. The lining material has an unknown impedance distribution $\zeta(x)$, as shown. The uniform flow of speed u_0 is subsonic and flows from left to right. The problem is to determine the impedance of the material as a function of the flow Mach number from the measured boundary data.

Steady-state acoustic pressure waves that propagate within the duct shown in figure 1 satisfy the equations⁷

$$i\omega p + u_0 \frac{\partial p}{\partial x} = -\rho_0 c_0^2 \left(\frac{\partial u}{\partial x} + \frac{\partial v}{\partial y} \right) \quad (1)$$

$$i\omega u + u_0 \frac{\partial u}{\partial x} = -\frac{1}{\rho_0} \frac{\partial p}{\partial x} \quad (2)$$

$$i\omega v + u_0 \frac{\partial v}{\partial x} = -\frac{1}{\rho_0} \frac{\partial p}{\partial y} \quad (3)$$

Physically, these three continuity equations represent the linearized conservation equations for mass, axial momentum, and transverse momentum, respectively, in the flowing fluid. For this paper, equations (1)-(3) are conveniently combined into a single, second order partial differential equation on the acoustic pressure field

$$(1 - M_0^2) \frac{\partial^2 p}{\partial x^2} + \frac{\partial^2 p}{\partial y^2} - 2ikM_0 \frac{\partial p}{\partial x} + k^2 p = 0 \quad (4)$$

Before a solution to the acoustic field can be obtained and the unknown impedance educed, boundary conditions must be prescribed.

Along the source plane of the duct, $x = 0$, the acoustic pressure $p_s(y)$ is assumed to be measured

$$p = p_s \quad (5)$$

Along the rigid upper wall the normal component of acoustic particle velocity must vanish (i.e., $v = 0$), thus

$$\frac{\partial p}{\partial y} = 0 \quad (6)$$

At the duct termination ($x = L$) the ratio of the acoustic pressure to the normal component of acoustic particle velocity must equal the measured exit impedance, $\zeta_{\text{exit}}(y)$

$$\frac{p}{u} = \zeta_{\text{exit}} \quad (7)$$

which when substituted into the axial momentum equation (2) and simplified gives

$$\frac{\partial p}{\partial x} = \frac{-ikp}{[M_0 + \zeta_{\text{exit}}]} \quad (8)$$

The lower wall locally reacting condition gives⁸

$$v = -\beta p - \frac{M_0}{ik} \frac{\partial}{\partial x} [\beta p] \quad (9)$$

Equation (9) can be conveniently substituted into the transverse momentum equation (3) to yield

$$\frac{\partial p}{\partial y} = ik\beta p + 2M_0 \frac{\partial}{\partial x} [\beta p] + \frac{M_0^2}{ik} \frac{\partial^2}{\partial x^2} [\beta p] \quad (10)$$

Equations (4), (5), (6), (8), and (10) form a well-posed boundary value problem that can be solved numerically to determine uniquely the upper wall pressures for a given admittance function, $\beta(x)$. Conversely, if the upper wall pressures at $x = x_1, x_2, x_3, \dots, x_m$ are measured along with $p_s(y)$, $p(x, H)$ and $\zeta_{\text{exit}}(y)$, then a unique test liner impedance function exists that will reproduce these wall pressures. Thus, the goal of this paper is to devise a procedure for educing this unknown liner impedance function.

Numerical Method

The numerical method chosen to solve the governing equation coupled with the boundary conditions closely parallels that used in the earlier paper⁴. However, the convective effects of the flow have introduced second derivative terms in the wall admittance boundary condition (10), so that the basis functions used in the finite-element method must be such that both the acoustic pressure p and its axial derivative (i.e., $\frac{\partial p}{\partial x}$) is continuous at the lower boundary (i.e., cubic element or higher must be used).

When applied to the current acoustic problem, the finite-element method may be interpreted as an approximation to the continuous acoustic field as an assemblage of rectangular elements (see figure 2). Here N nodes are assumed in the axial and M nodes are assumed in the transverse direction of the duct. A typical rectangular element with width a and height b , shown in figure 3, consists of four local node numbers labeled 1, 2, 3, and 4, respectively. The objective is to obtain the unknown acoustic pressures at

the nodes of each of the $(M - 1)(N - 1)$ elements. Galerkin's finite-element method is used to minimize the field error. The field error function is defined as

$$E(x, y) = (1 - M_0^2) \frac{\partial^2 p}{\partial x^2} + \frac{\partial^2 p}{\partial y^2} - 2ikM_0 \frac{\partial p}{\partial x} + k^2 p \quad (11)$$

Within each element the acoustic pressure p , is

$$p(x, y) = \sum_{I=1}^{I=16} N_I(x, y) \Phi_I \quad (12)$$

The basis $N_I(x, y)$ and nodal coefficients Φ_I are identical to those used in the quadrilateral elements for plate bending (see for example reference 9) and are not written explicitly here.

The variable exit impedance $\zeta_{\text{exit}}(y)$ and wall admittance $\beta(x)$ are represented in a similar manner along each boundary element:

$$\begin{aligned} \zeta_{\text{exit}}(y) &= \zeta_{\text{exit}}(y_J) f_1(y, b) + \zeta_{\text{exit}}(y_{J+1}) f_3(y, b) \\ &\quad \zeta'_{\text{exit}}(y_J) f_2(y, b) + \zeta'_{\text{exit}}(y_{J+1}) f_4(y, b) \end{aligned} \quad (13)$$

$$\begin{aligned} \beta(x) &= \beta_{I1} f_1(x, a) + \beta_{I2} f_2(x, a) \\ &\quad + \beta_{I3} f_3(x, a) + \beta_{I4} f_4(x, a) \end{aligned} \quad (14)$$

$$\begin{aligned} f_1(x, a) &= 1 - 3x^2/a^2 + 2x^3/a^3 \\ f_2(x, a) &= x(x/a - 1)^2 \\ f_3(x, a) &= (x^2/a^2)(3 - 2x/a) \\ f_4(x, a) &= (x^2/a)(x/a - 1) \end{aligned} \quad (15)$$

where β_{Iq} are unknown coefficients to be determined. For $(N - 1)$ columns of elements, $4(N - 1)$ coefficients must be determined. Ideally, the solution to the sound field is obtained when the field error $E(x, y)$ is identically zero at each point of the domain. Thus the field error function is made to be orthogonal to each basis function $N_I(x, y)$. Contributions to the minimization of the field error function from a typical element are

$$\int EN_I dA \quad (16)$$

Each second derivative term in the integrand of equation (16) is integrated by parts and the admittance boundary conditions are incorporated at the element level just as in reference 4.

The contribution to the minimization of the field error for each element is expressed in matrix form as

$$\int EN_I dA = [A^{[I, J]}] \{\Phi^{[I, J]}\} \quad (17)$$

at four target centerline Mach numbers (i.e., 0.0, 0.1, 0.3, 0.5).

Acoustic waves are propagated from left to right, across the surface of the test specimen, and into a termination section designed to minimize reflections over the frequency range of interest. Two 6 mm condenser-type microphones are flush-mounted in the test section, one at a fixed location on the side wall, and the other on an axial traverse bar. A 13 mm wide precision-machined slot in the top wall of the flow impedance tube allows this axial traverse bar to traverse the test section length by means of a computer controlled digital stepping motor. The fixed location microphone is used to provide a reference.

The source plane acoustic pressure and exit plane impedance are functions of position along these planes. Therefore, transverse probe microphones should be used to measure this data when the test specimen is installed. This facility is not designed to easily accommodate a transverse probe microphone since it is intended to operate below the cut-on of any higher order modes. The experiment was therefore carefully designed to minimize higher order mode effects along the source and exit planes. Almost all the data for the duct propagation model were obtained from measurements made by the upper wall traversing microphone. It should be noted that because of the sound absorbing properties of the liner, it is not possible to avoid high order mode effects in the liner region. The high order mode effects and reflections will initiate in the vicinity of the leading and trailing edge of the specimen.

To avoid the need for a transverse probe, the source plane was chosen 200 mm upstream of the leading edge of the test specimen in the hardwall section of the duct, and the source frequency was kept below the cut-on of higher order hardwall modes. Higher order mode effects caused by the installation of the test specimen are expected to decay upstream of the leading edge of the test specimen. Therefore, the source pressure at each point along the source plane was set to the value measured at the upper wall source location. A similar procedure was applied at the exit plane. The switched, two microphone method developed in ref. 10 was used, with a hardwall test specimen installed to obtain the exit impedance.

Impedance Eduction Technique

The measured data $p_s(y)$ and $\zeta_{\text{exit}}(y)$, provide a set of consistent boundary data for testing the impedance eduction technique. The solution to equation (19) gives the upper wall acoustic pres-

sure as a function of the undetermined coefficients β_{Iq} . These coefficients are determined from the measured upper wall acoustic pressures. The procedure is to determine values of these coefficients such that the upper wall pressure solution obtained from equations (19) reproduces the measured upper wall acoustic pressures $p(x_l, H)$. This is achieved by minimizing the objective function:

$$\psi(\beta_{Iq}) = \frac{1}{m} \sum_{l=1}^m |p(x_l, H) - P_{\text{FE}}(x_l; \beta_{Iq})| \quad (22)$$

Note that this positive definite-objective function may be interpreted as the difference between the known acoustic wall pressure and that computed by the finite element method.

Because the optimization algorithm makes use of the objective function gradient to find its minimum, and this function is available only in numerical form (i.e., as a finite element solution of equation (19)), Stewart's adaptation of the Davidon-Fletcher-Powell (SDFP) optimization method is used to obtain the minimum.¹¹

Description of Test Liners

Results in the following section test SDFP's ability to converge to the known normal incidence admittance of a solid steel plate and to the measured normal incidence admittance of two soft test liners. The soft test liners were chosen because their admittances are expected to be fairly insensitive to the flow Mach number and sound pressure levels. Baseline admittance spectra for these two liners were established therefore, from measurements in a conventional normal incidence impedance tube. The three liners, shown schematically in figure 5, are intended for validation purposes only and are described further below:

- a) This liner is actually a stainless steel insert that continues the hard-wall condition of the flow duct. It provides a baseline condition to establish zero admittance.
- b) This liner consists of a ceramic structure of parallel, cylindrical channels, .635 mm in diameter, embedded in a ceramic matrix. The 85 mm depth channels (i.e., $d=85$ mm) run perpendicular to the exposed surface to provide a surface porosity of 57 percent and resonant frequency of 1000 Hertz. The channels are rigidly terminated such that each is isolated from its neighbor to ensure a locally reacting structure.
- c) The final test liner is a 76 mm depth (i.e., $d=76$ mm) slot liner composed of 65 slot cavities

with a resonant frequency of 1,150 Hertz. The slot liner consists of 66 aluminum parallel plates that are placed approximately 6 mm apart. A 100 MKS Rayls fibermetal facesheet is bonded to the surface of the liner.

Note that the experimentally determined normal incidence admittance for the slot liner is prone to somewhat more systematic error than is the case for the ceramic liner. This possible loss of accuracy is attributable to the 51 mm width of the standing wave tube (SWT) apparatus not being precisely equal to a multiple of the slot width and to a mounting procedure that may have not provided as nearly an airtight seal as was the case for the more conventional “ceramic tubular construction.”

Results and Discussion

Computer Code

An in-house computer code that implements the SDFP impedance eduction or “measurement” method has been developed. Solution of the finite-element matrix equation and the minimization of the objective function are performed by using highly developed software packages that are available at “NASA Langley Research Center.” Results are computed on a DEC-Alpha work station. An evenly spaced 251x11 grid is used ($N = 251$ and $M = 11$) in the finite-element discretization for all calculations. This grid ensures that a minimum of 10 elements per axial wavelength is used in the finite-element discretization at the highest frequency of interest. Results are presented for six selected frequencies (.5, 1.0, 1.5, 2.0, 2.5 and 3.0 kHz) and four targeted centerline Mach numbers (0.0, 0.1, 0.3, and 0.5). All calculations are performed at standard atmospheric conditions using the duct geometry of the Langley Flow Impedance Tube Facility (i.e., $H = 51$ mm, $L = 861$ mm, $L_1 = 200$ mm, and $L_2 = 611$ mm). The undetermined coefficients β_{Iq} consistent with the measured acoustic pressure distribution on the upper wall are returned by the SDFP optimization algorithm. Note that all results are given in terms of the admittance function $\beta(x)$, the corresponding impedance function is obtained from its reciprocal (i.e., $\zeta(x) = 1/\beta(x)$).

The objective function for all results to follow is constructed using all of the 34 upper wall points (i.e., $m = 34$). Because all of the liners tested have constant wall admittance functions β , the number of optimization variables were reduced from $8(N - 1)$ to only two. This constant admittance function, β , is obtained from equation (14) by setting

$$\beta_{I2} = \beta_{I4} = 0 + 0i, \quad \beta_{I1} = \beta_{I3} = \beta \quad (23)$$

Thus, the wall objective function is a function only of the uniform admittance, β (i.e., $\psi = \psi(\kappa, \sigma)$). Here κ is the conductance and σ the susceptance of the test liner (i.e., $\beta = \kappa + i\sigma$). It should be noted that the admittance spectrum computed for each flow Mach number consumed less than 12 minutes of CPU time on the work station.

Rigid Test Liner

Figure 6 shows the SDFP educed admittance spectrum for the rigid test liner for each targeted centerline Mach number. Educed conductance and susceptance values for this test liner are not only independent of the flow Mach number but are in excellent agreement with the “known” values of a solid surface (i.e., conductance and susceptance values for a solid surface are zero). The accuracy of the SDFP educed susceptance spectrum is slightly less accurate than the educed conductance spectrum.

Ceramic Test Liner

Comparisons between the SDFP educed admittance spectrum and that measured in the standing wave impedance tube (SWT) for the ceramic test liner is shown in figure 7. The agreement between SDFP and the measured spectrum agree well except at the resonant frequency (i.e., 1.0 kHz) of the ceramic material. At the resonant frequency, there is generally a decrease in the accuracy of the measured data obtained with the highly tuned liner installed due to a signal to noise problem. This probably accounts for the discrepancy at 1.0 kHz. Note that the admittance spectrum is minimally influenced by the flow Mach number except at the lowest frequency of interest (i.e., .5 kHz). The dependency of the admittance upon the flow Mach number at .5 kHz was not expected and is still under investigation. The agreement between the measured and SDFP computed spectrum becomes slightly worse with increasing Mach number. This is expected since the mean boundary layer thickens with increasing Mach number and the uniform flow assumption is violated.

Slot Liner

Figure 8 shows comparisons between the admittance spectrum measured in the standing wave tube with that determined by SDFP for the slot liner. The reader is reminded that the measurements shown in the figure are more subject to systematic error than were those obtained for the ceramic liner. There is a large discrepancy between the measured and the SDFP educed admittance (especially the susceptance) at the frequency closest to the resonant frequency of the slot liner (i.e., 1.0 kHz). Otherwise the agreement between the measured and SDFP

duced admittance spectrum is generally good. Note the unexpected result, that the susceptance of the slot liner is a function of the flow Mach number at a frequency of .5 kHz.

Conclusions

Based on the results of this work, the following specific conclusions are drawn:

1. The development of the SDFP impedance education method represents a significant step forward in impedance “measurement” technology in flow. The method extends impedance measurement techniques to variable impedance liners and is extendable to shearing mean flows.
2. The SDFP method reproduces “measured” normal incidence admittance spectra for a rigid and two soft test liners in flow except at the resonant frequency, where the quality of the measured data was poor due to a signal to noise problem cause by the highly tuned liners.
3. The admittance of the soft test liners show a dependence upon the flow Mach only at a frequency of .5 kHz. The dependency of the admittance on the flow Mach number even at .5 kHz was unexpected and is under further investigation.
4. The success of the SDFP impedance education method motivates its extension to include the refractive effects of the flow, and this effort is currently underway.

References

¹Armstrong, D. L., Beckemeyer, R. J., and Olsen, R. F., “Impedance Measurements of Acoustic Duct Liners With Grazing Flow,” Paper presented at the 87th Meeting of the Acoustical Society of America, New York, NY, 1974.

²Watson, W. R., “A Method for Determining Acoustic-Liner Admittance in a Rectangular Duct With Grazing Flow From Experimental Data,” NASA TP-2310, 1984.

³Watson, W. R., “A New Method for Determining Acoustic-Liner Admittance in Ducts With Sheared Flow in Two Cross-Sectional Directions,” NASA TP-2518, 1985.

⁴Watson, Willie R., Jones, Michael G., Tanner, Sharon E., and Parrott, T. L., “A Finite Element Model for Extracting Normal Incidence Impedance in Nonprogressive Acoustic Wave Fields.” *Journal of Computational Physics*, vol. 125, pp. 177–186, 1996.

⁵Watson, Willie R., Jones, Michael G., Tanner, Sharon E., and Parrott, T. L., “Validation of a Numerical Method for Extracting Liner Impedance.” *AIAA Journal*, vol. 34, No. 3, pp. 548–554, 1996.

⁶Watson, Willie R., Tanner, Sharon E., and Parrott, T. L., “Optimization Method for Educing Variable-Impedance Liner Properties” *AIAA Journal*, vol. 36, No. 1, pp. 18–23, 1998.

⁷Kraft, R.E., “*Theory and Measurements of Acoustic Wave Propagation In Multi-Segmented Rectangular Ducts*,” P.h.D. Thesis, University of Cincinnati, 1976.

⁸Myers, M.K., “On The Acoustic Boundary Condition In The Presence Of Flow,” *Journal Of Sound And Vibrations*, Vol. 71 No. 3 , pp. 429-434, 1980.

⁹Chandrakant S.; and Abel, John F., “Introduction To The Finite Element Method,” Van Nostrand Reinhold Company, New York, N.Y. 1972.

¹⁰Jones, Michael G., and Parrott, Tony L., “Evaluation of a Multi-point Method for Determining Acoustic Impedance” *Mechanical Systems and Signal Processing*, vol 3, No. 1, pp. 15–35, 1989.

¹¹Stewart, G.W. III: A Modification of Davidon’s Minimization Method to Accept Difference Approximations of Derivatives. *Journal of ACM*, vol. 14, No. 1, pp 72-83, January 1967.

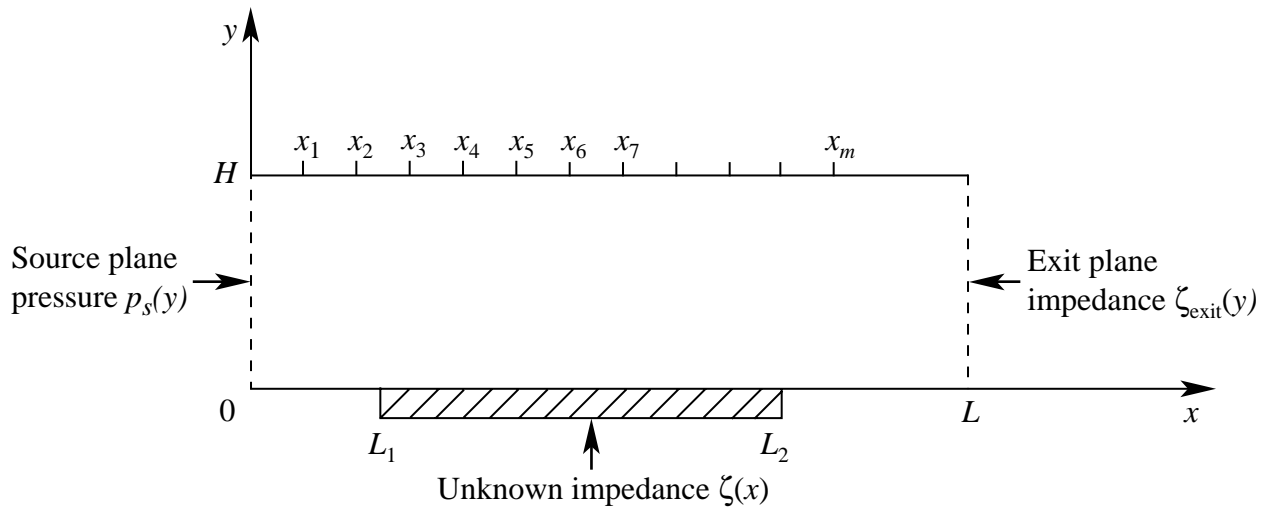


Fig. 1 Two Dimensional Duct and coordinate system.

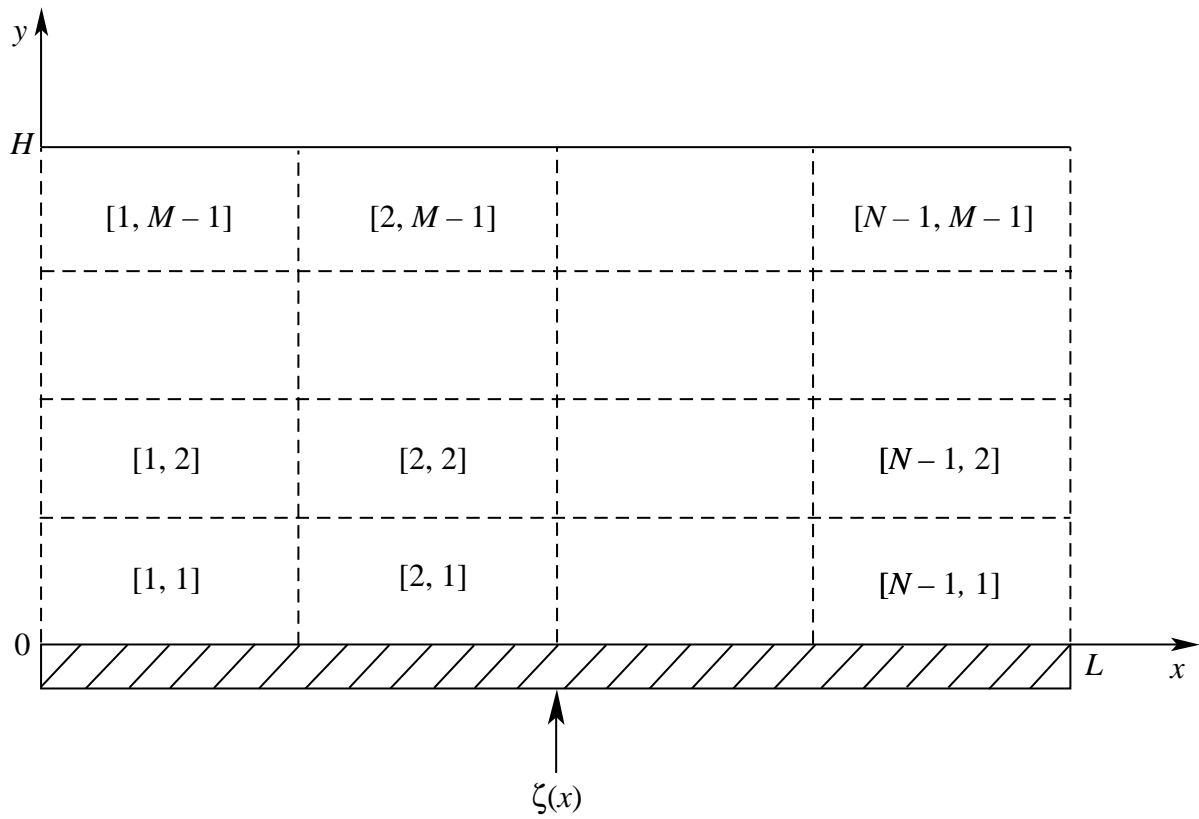


Fig. 2 Finite element discretization of the two dimensional duct.

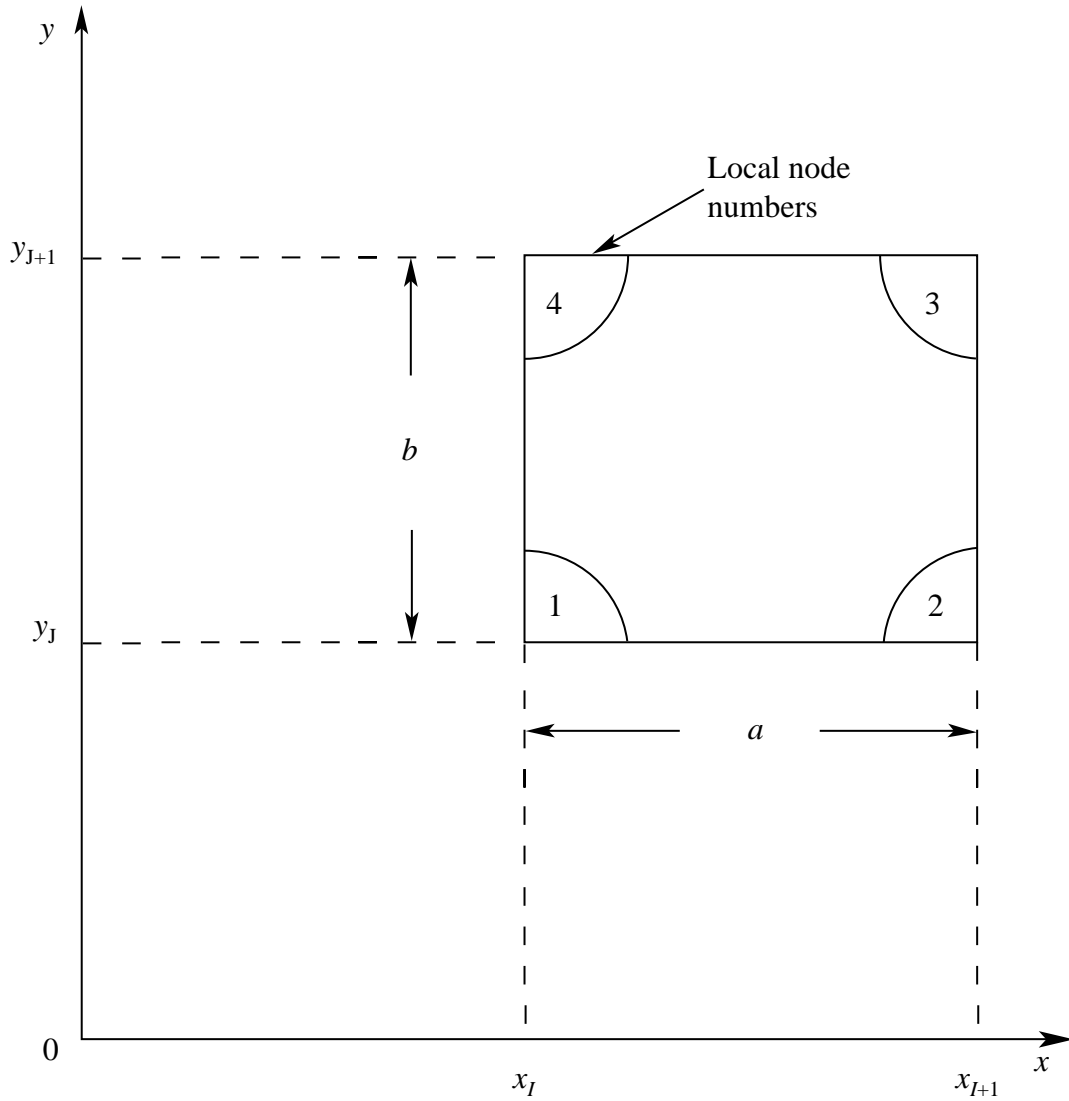


Fig. 3 A typical finite element and local node numbering system.

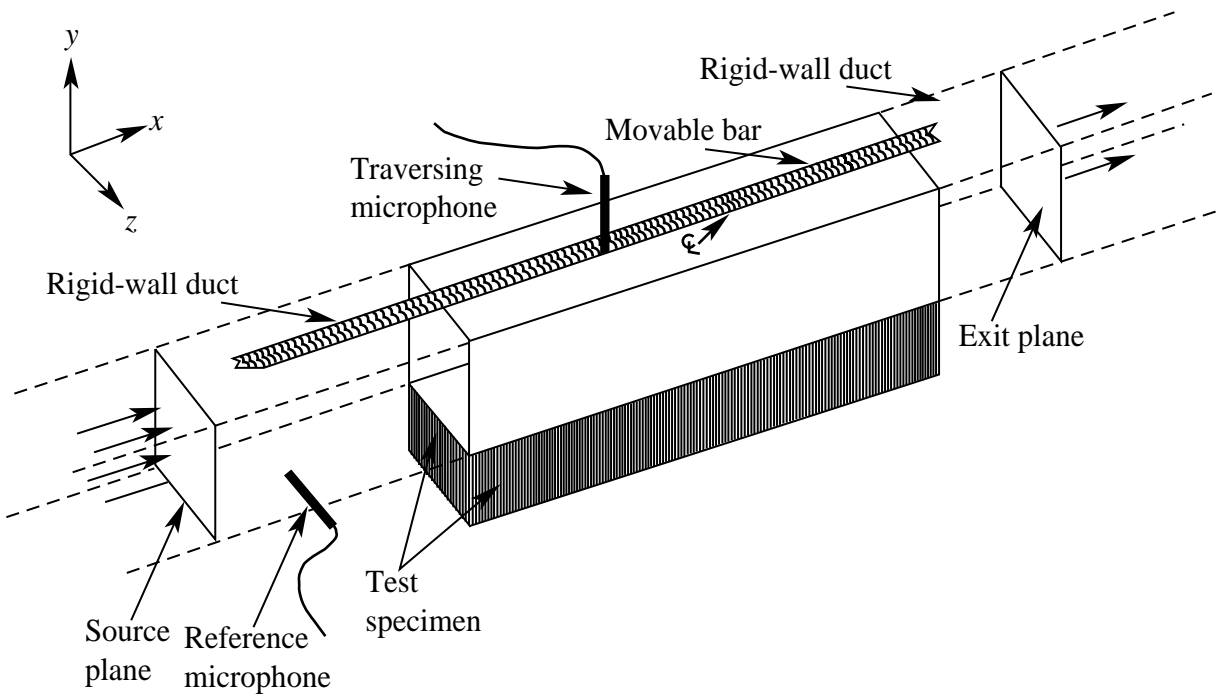


Fig. 4 Schematic of Langley Flow Impedance Tube.

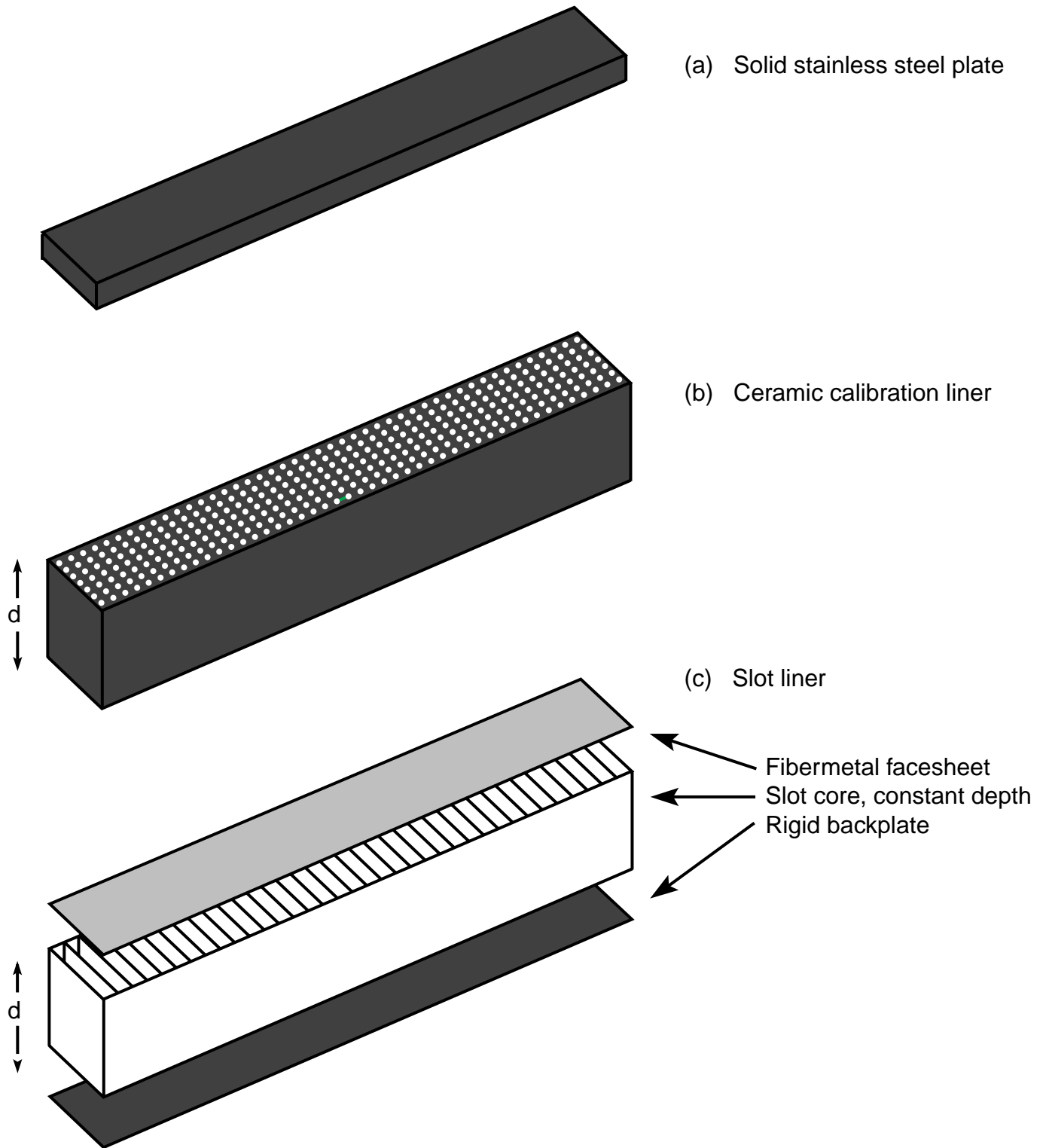


Fig. 5 Schematic of test liners.

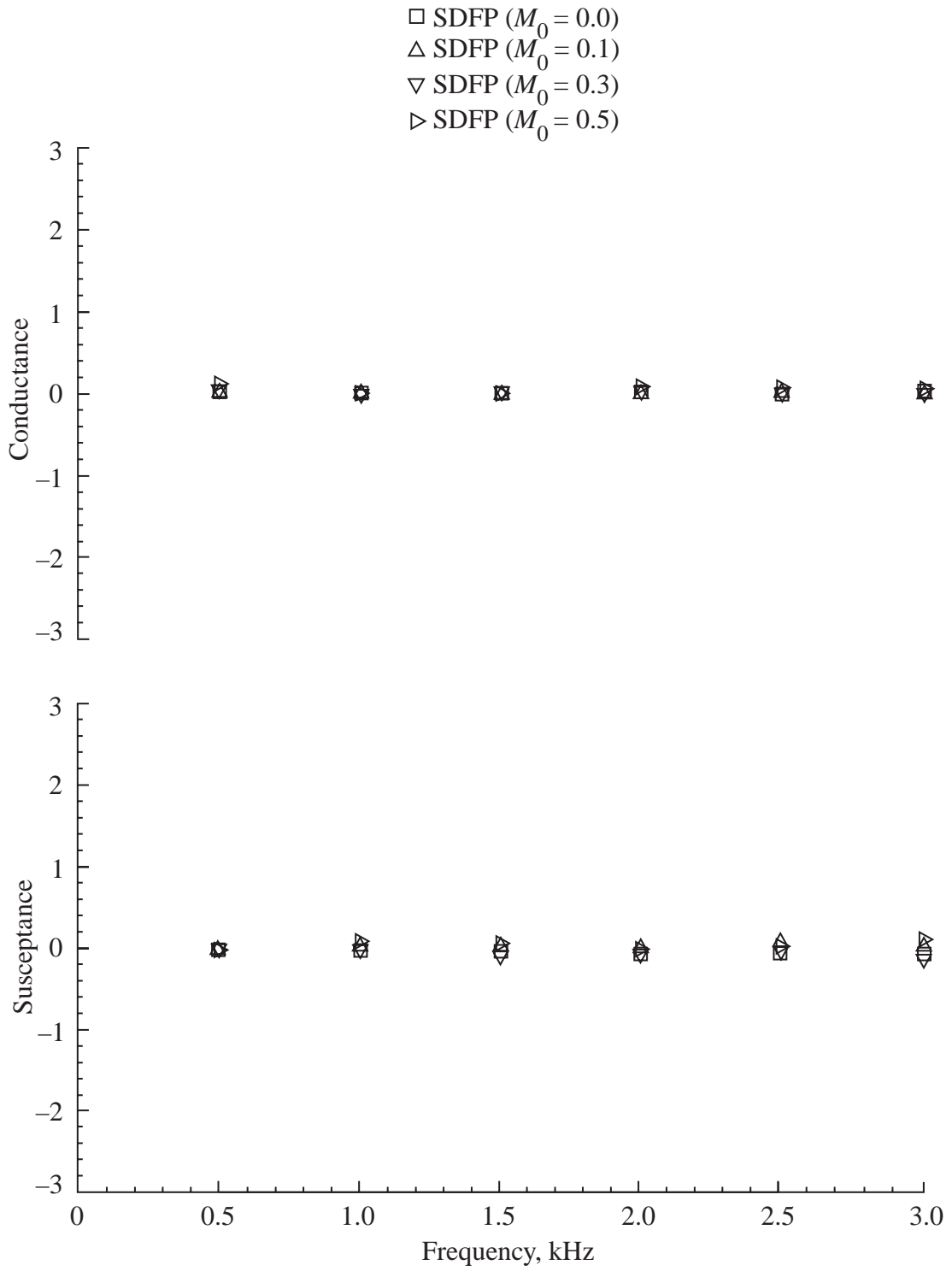


Fig. 6 Educated admittance spectrum for the rigid test liner.

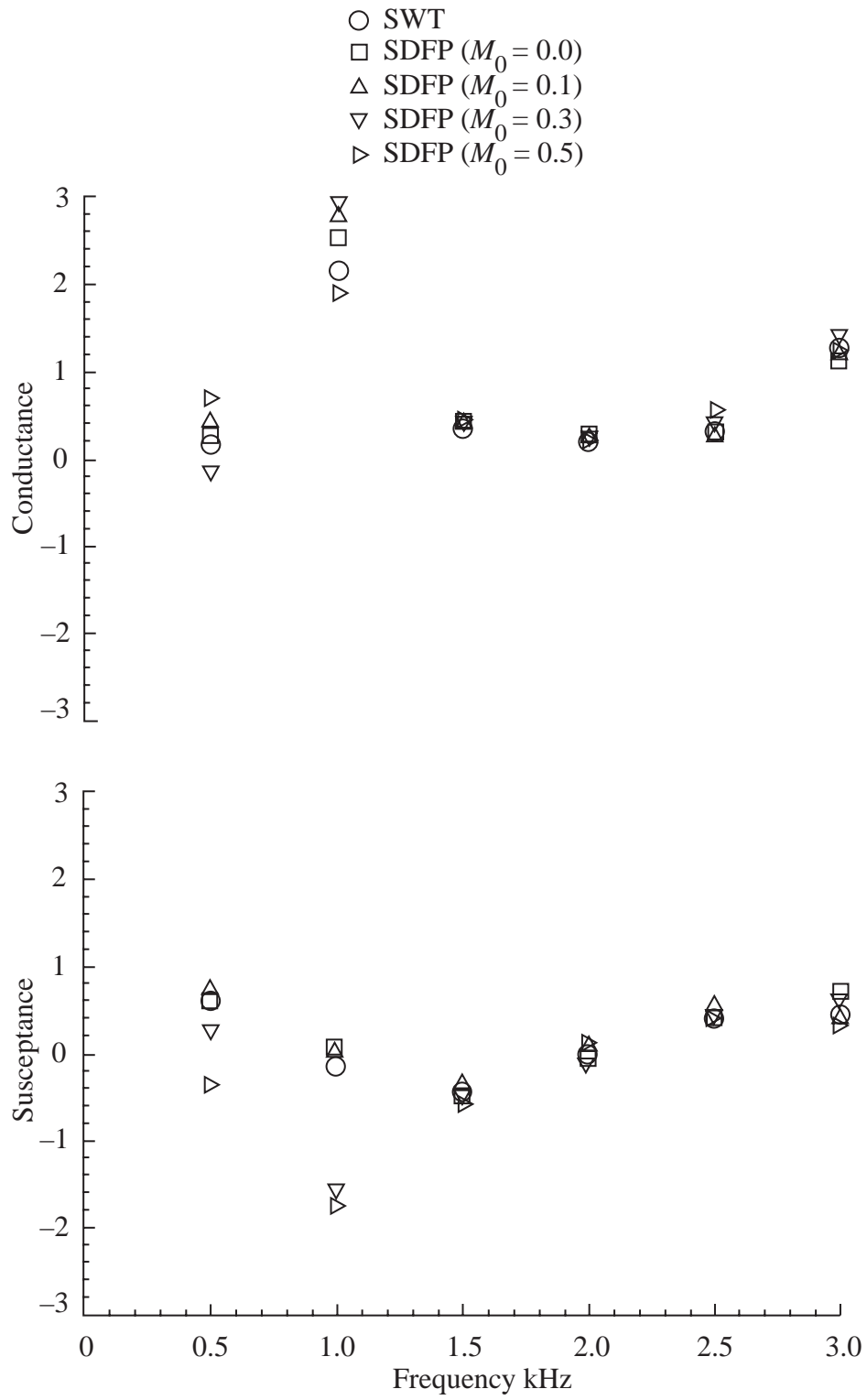


Fig. 7. Comparison of the admittance spectrum for the ceramic calibration liner.

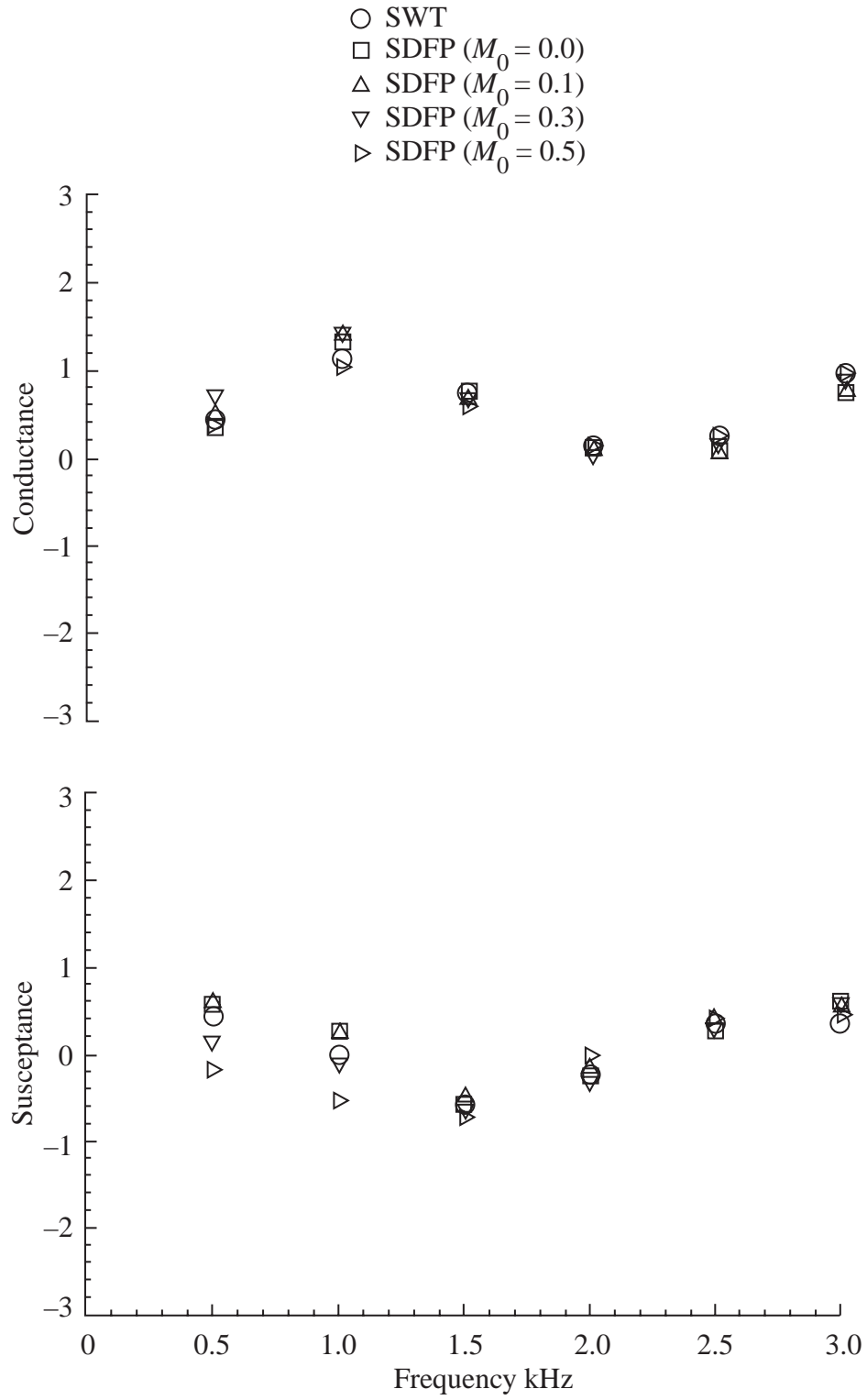


Fig. 8. Comparison of the admittance spectrum for the slot liner.